Supporting Information

Highly Effective Solar CO_2 Fixation via Photocatalytic Carboxylation of Aromatic Amines with Carbon Dioxide over Covalent Organic Framework (COF) as a Photocatalyst

Chandani Singh,[a] Jae Young Kim,[a] No-Joong Park,[a] Rajesh Kumar Yadav,[b] and Jin-Ook Baeg*[a]

[a]CO_2 Energy Research Center, Korea Research Institute of Chemical Technology (KRICT), 100 Jang-dong, Yuseong, Daejeon 34114, Republic of Korea

E-mail: jobaeg@krict.re.kr

[b]Department of Chemistry and Environmental Science, Madan Mohan Malaviya University of Technology, Gorakhpur, Uttar Pradesh, 273016, India

Table of Contents

1. General information

^{1}H NMR (500 MHz) spectra were recorded on a Bruker AVANCE II+ 500 MHz NMR spectrometer with tetramethylsilane (TMS; δ = 0) as the internal standard. Multiplicities are reported as follows: singlet (s), doublet (d), doublet of doublets (dd), triplet (t), quartet (q), and multiplet (m). UV–vis diffuse reflectance spectra (UV–vis DRS) of solid COFs were recorded by SCINCO S-4100 diffuse reflectance-ultraviolet/visible (DR-UV/Vis) spectrophotometer and UV-visible spectra of liquid samples were recorded on a Shimadzu UV-1800 spectrophotometer. Fourier transform infrared (FTIR) spectra of liquid compounds were obtained on Bruker ALPHA-T Infrared Spectrometer (IR). High-Resolution X-ray diffraction (HR-XRD) data were carried out by using the Rigaku SmartLab High-Resolution X-ray Diffractometer (HR-XRD). The X-ray diffraction patterns were recorded in the range of 2θ = 2–70° with Cu Kα radiation (λ = 1.5406 Å) at 45 kV and 200 mA. X-ray photoelectron spectroscopy (XPS) spectra were recorded on an AXIS SUPRA (KRATOS) using a monochromatic Al-Kα X-ray source at 15KeV. Field-emission scanning electron microscopy (FE-SEM) images were recorded on a Carl Zeiss Æ©IGMA HD FESEM instrument at 10 keV. The energy dispersive X-ray studies (EDX) were carried out on a Bruker Quantax 200 Energy Dispersive X-ray Spectrometer equipped with a Si Drift Detector (SDD). Transmission Electron Microscopy (TEM) images were taken on UC-EF-TEM operated at an accelerating voltage of 200 kV. Thermogravimetric analysis (TGA) was conducted on a Scinco analyzer from 30 to 900 °C under an N_2 atmosphere with a ramp rate of 10 °C min^{-1}. Nitrogen adsorption isotherms analysis was carried out on the ASAP2420 instrument at 77 K using a liquid nitrogen bath. Before gas adsorption treatment sample was degassed for 12 h at 150 °C under a vacuum. Photocurrent and EIS were also performed on a CHI 750E electrochemical analyzer.

2. Experimental section:

2.1. Materials:

Hexamethylenetetramine (HMTA), trifluoroacetic acid (TFA), mesitylene, dioxane, tert-butyl nitrite, anhydrous CH_3CN, anhydrous MeOH, triethylamine (TEA), nickel (II) chloride hexahydrate and dimethylglyoxime were purchased from Sigma Aldrich. Anhydrous phloroglucinol, 3, 7-diamino-2, 8-dimethyl dibenzothiophene sulfone (DAMS), 2,3,5,6-tetramethyl-1,4-phenylenediamine (TMPA) and 1,8-diazabicyclo [5.4.0] undec-7-ene (DBU) were purchased from TCI, Korea. All aromatic amine derivatives were purchased from Sigma Aldrich and TCI, Korea. All the solvents used in the experiment were of HPLC grade and used without further purification.

2.2. Synthesis of 1,3,5-triformylphloroglucinol (Tp):

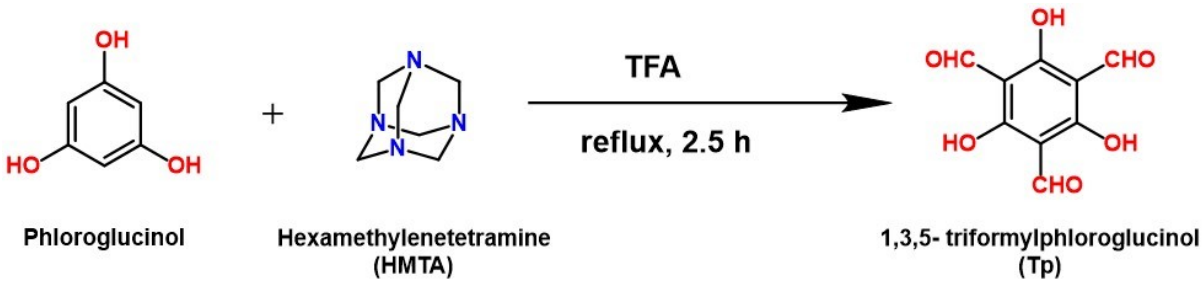

Scheme S1. Synthesis of 1,3,5-triformylphloroglucinol (Tp) from phloroglucinol.

To anhydrous phloroglucinol (5 g, 40 mmol) and hexamethylenetetramine (HMTA) (12.5 g, 89.5 mmol), 75 mL trifluoroacetic acid (TFA) was slowly added at 0°C under inert atmosphere. After complete addition, the reaction mixture was heated at 100 °C for 2.5 h (Scheme S1). Then, 120 mL of 3 M HCl was added after cooling the reaction mixture to around 50 °C, and then heated at 100 ºC for 1 h. After cooling to room temperature, the

solution was filtered through celite, extracted with dichloromethane (350 mL), dried over magnesium sulfate, and filtered. Rotary evaporation of the solution afforded an off-white powder. A pure sample was obtained by washing with hot EtOH (1.42 g, 16.7 %) (Figure S14). ^{1}H NMR (500 MHz, $CDCl_3$) δ 14.04 (s, 3H, OH), 10.08 (s, 3H, CHO).[1]

2.3. Synthesis of Ni $(dmg)_2$:

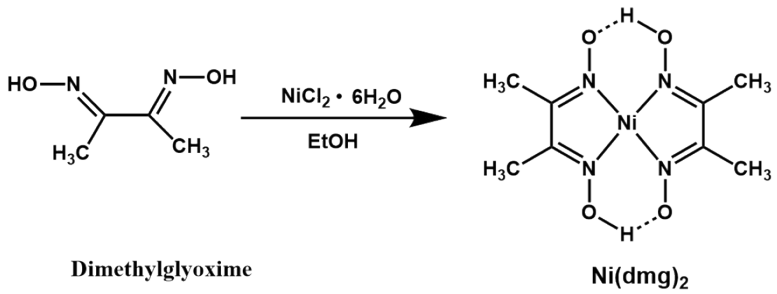

Scheme S2. Synthesis of bis (dimethyl glyoximato) nickel (II) [$Ni(dmg)_2$].

Dimethyl glyoxime (dmg, 2 mmol) was entirely dissolved in 10 mL of ethanol (EtOH) and then a solution of $NiCl_2 \cdot 6H_2O$ (1 mmol) in 10 mL of EtOH was added dropwise to the stirred solution at room temperature. After adding the entire solution, the stirring proceeded for 24 h (Scheme S2). Then the obtained precipitate was filtered and washed with glacial EtOH and Et_2O to give the desired product.

3. Results and discussion

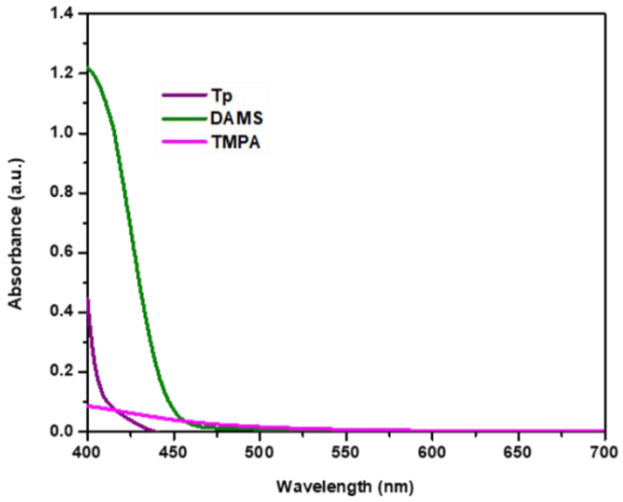

Figure S1. UV-visible spectra of Tp, DAMS, and TMPA monomers.

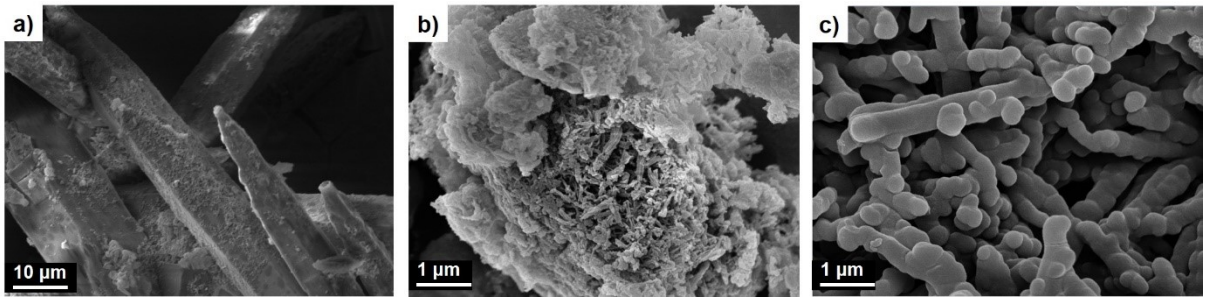

Figure S2. FE-SEM images of (a) Tp, (b) DAMS, and (C) TMPA monomers.

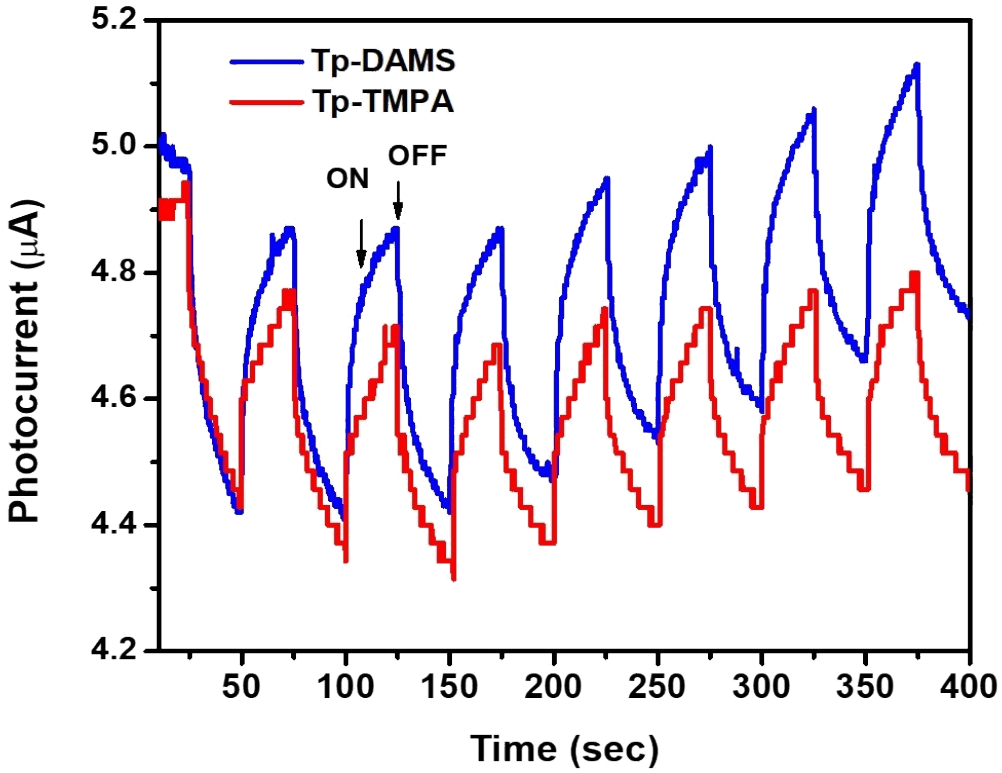

Figure S3. Transient photocurrent responses of Tp-DAMS and Tp-TMPA photocatalysts.

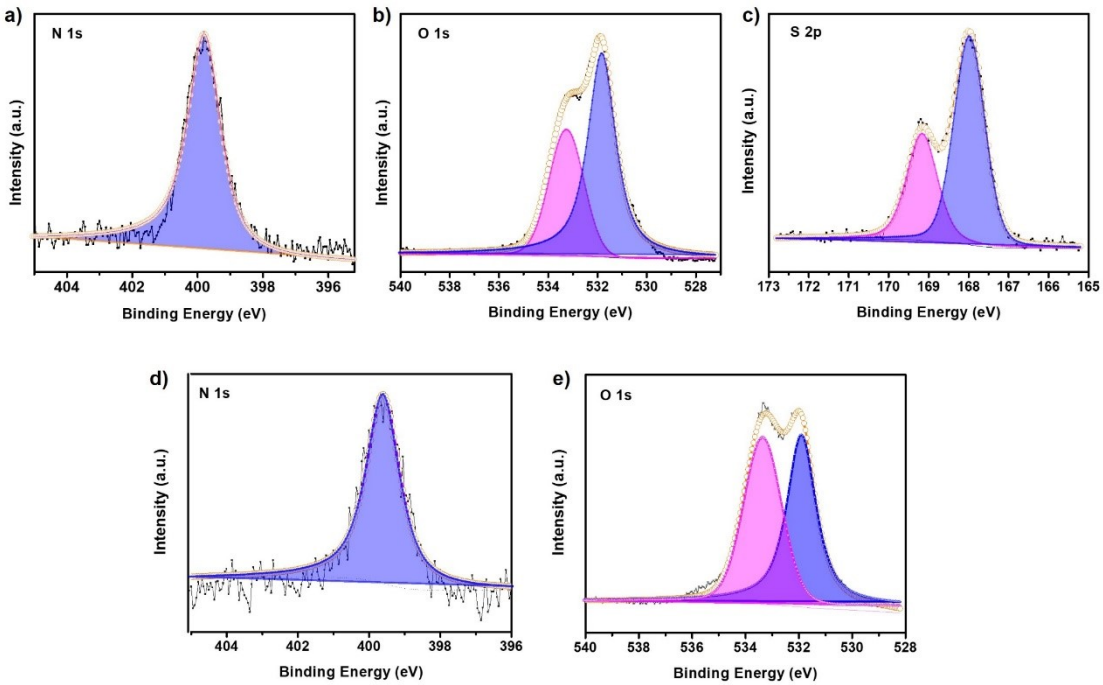

Figure S4. XPS data of Tp-DAMS (a-c) and Tp-TMPA (d, e) photocatalysts.

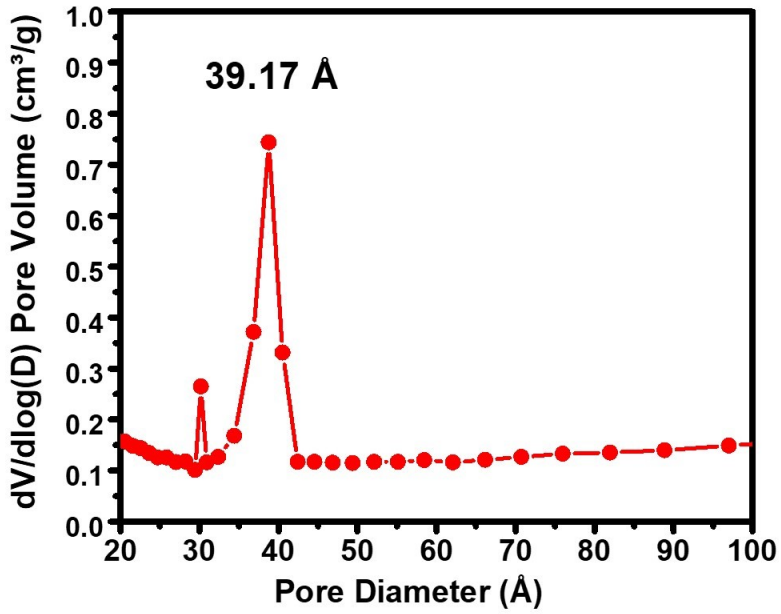

Figure S5. BET pore diameter of Tp-DAMS photocatalyst.

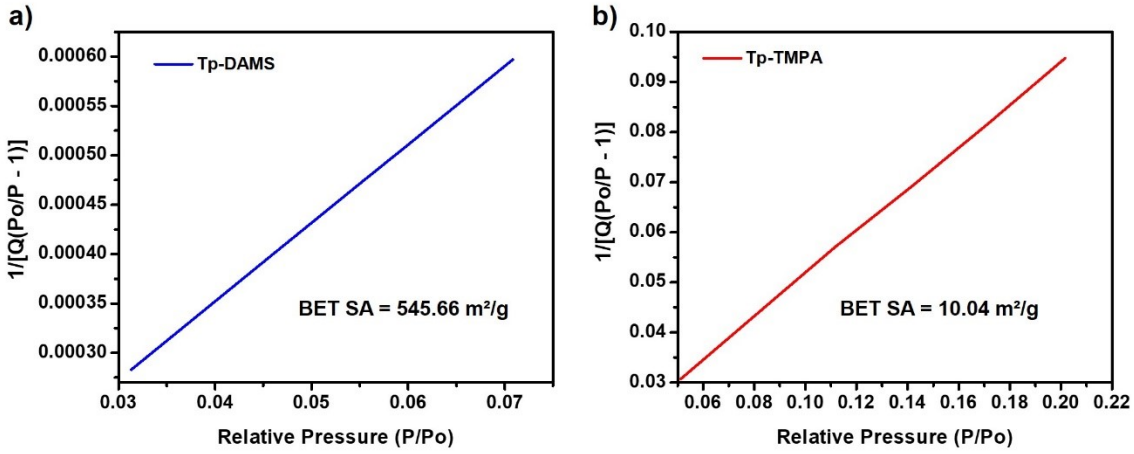

Figure S6. BET surface area plot of Tp-DAMS (a) and Tp-TMPA (b) photocatalysts.

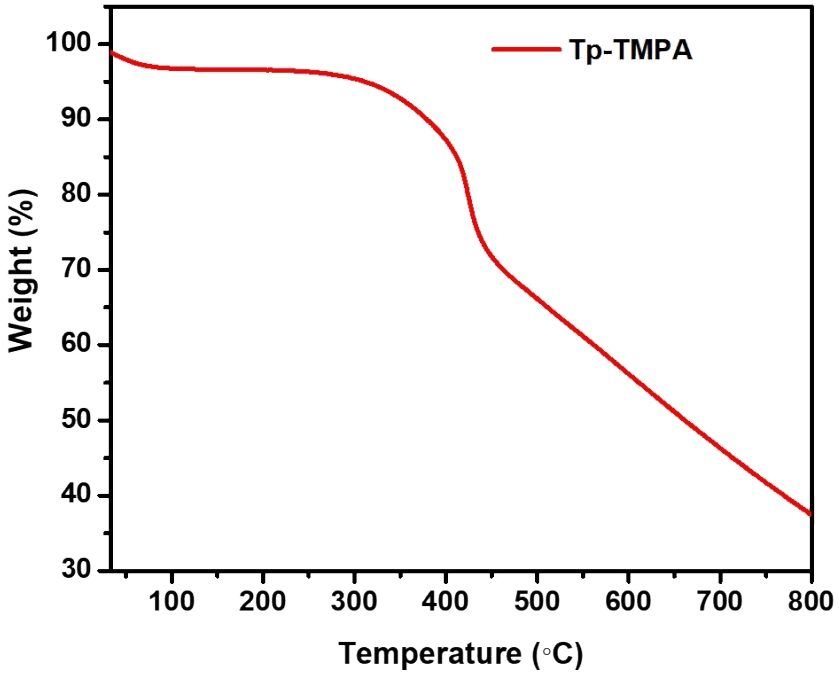

Figure S7. Thermogravimetric analysis (TGA) of Tp-TMPA photocatalyst.

Recyclability Test:

We have performed the recyclability test to probe the efficiency and stability of the Tp-DAMS photocatalyst (Figure S8). The recyclability test of the Tp-DAMS photocatalyst was carried out using the film form of COF, which was fabricated on the surface of the PET (polyethylene terephthalate) substrate. We have noticed a 95.0% yield of carboxylic acid after the 6th cycle, indicating the retention of high performance.

The recovered Tp-DAMS COF photocatalyst was characterized by FTIR, XRD, XPS, and TGA to demonstrate the robustness of the photocatalyst (Figure S9-S12). XRD pattern of pure PET, Tp-DAMS on PET substrate before, and after catalysis showed low and high intense diffraction peaks at 2θ angles of 23.0 (110) and 26.0° (100), which identified for PET crystalline structure (Figure S 9).[2-4] The intensity of the diffraction pattern of Tp-DAMS on PET substrate is lower than that of pure PET because of Tp-DAMS contribution to the overall XRD data. After catalysis, the crystalline diffraction peaks remain unchanged (Figure S9). Furthermore, the thermal stability of the Tp-DAMS COF photocatalyst also exhibited better stability (Figure S10). The FTIR and XPS analysis also confirmed the retention of chemical identity (Figures S11 and S12). The reused photocatalyst did not show an apparent

change at 1582 cm^{-1} (C=C), and 1273 cm^{-1} (C−N) in the FTIR spectrum after the catalysis (Figure S11). In the XPS spectrum, the C 1s, N 1s, O 1s, S 2s, and S 2p peaks also remained unchanged (Figure S12).

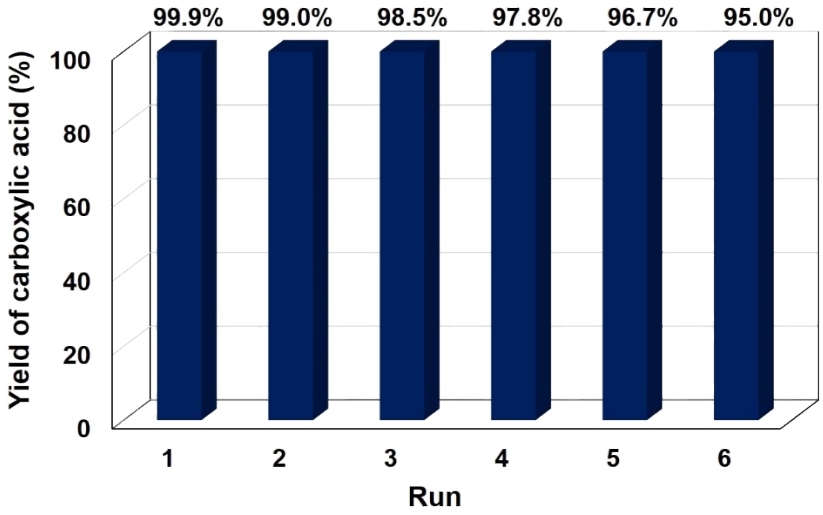

Figure S8. Recyclability of Tp-DAMS photocatalyst for aromatic carboxylic acid production up to six cycles. The photocatalysis was carried out using COF film photocatalyst by illuminating the quartz reactor containing aromatic amine (1 mmol), tert-butyl nitrite (1 mmol), and TEA (3 mmol) in 3 ml of CH_3CN. The aromatic carboxylic acid production was carried out in the presence of CO_2 under solar light irradiation. The COF film photocatalyst was washed and rinsed in CH_3CN for the next cycle.

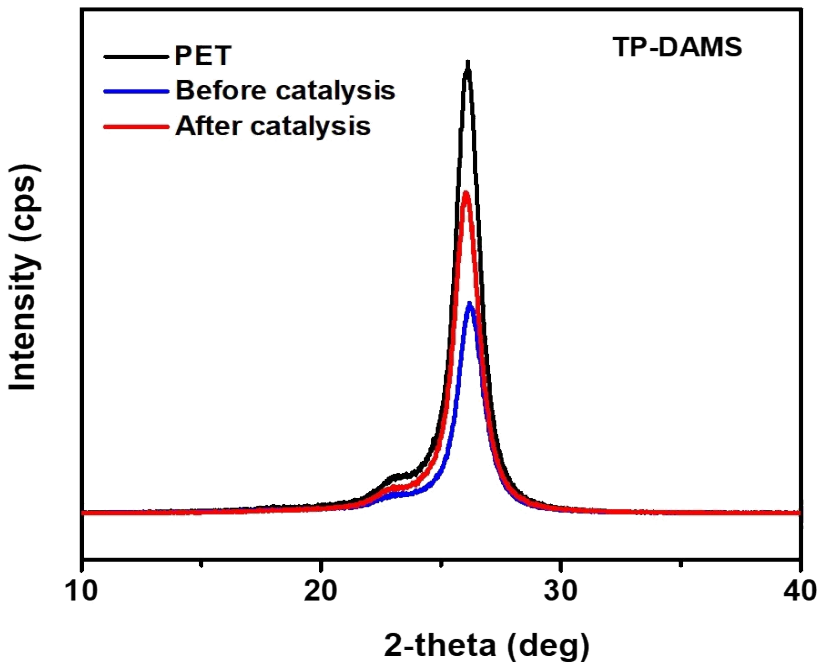

Figure S9. XRD pattern of PET and Tp-DAMS photocatalyst before and after the catalysis.

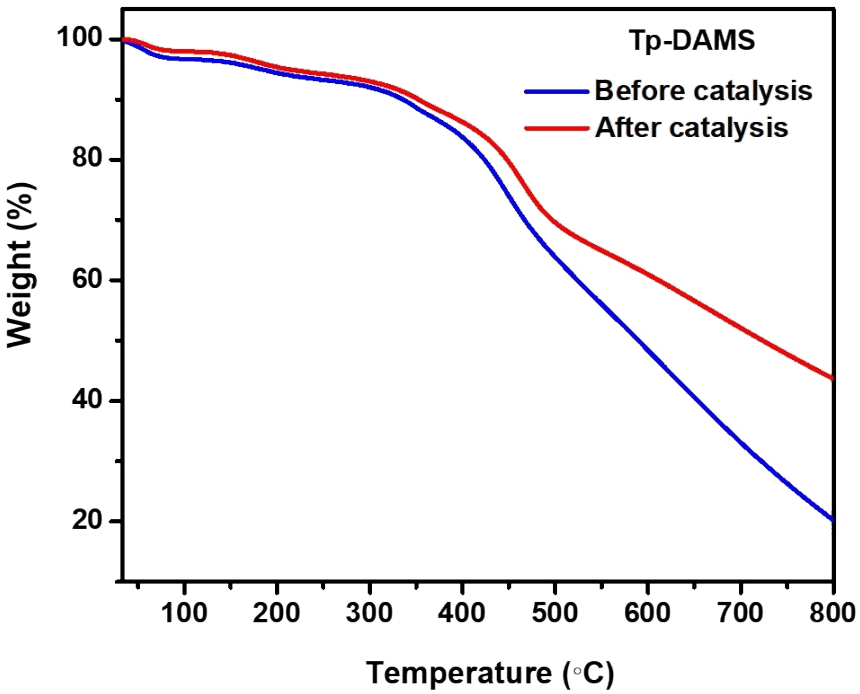

Figure S10. TGA analysis of Tp-DAMS photocatalyst before and after the catalysis.

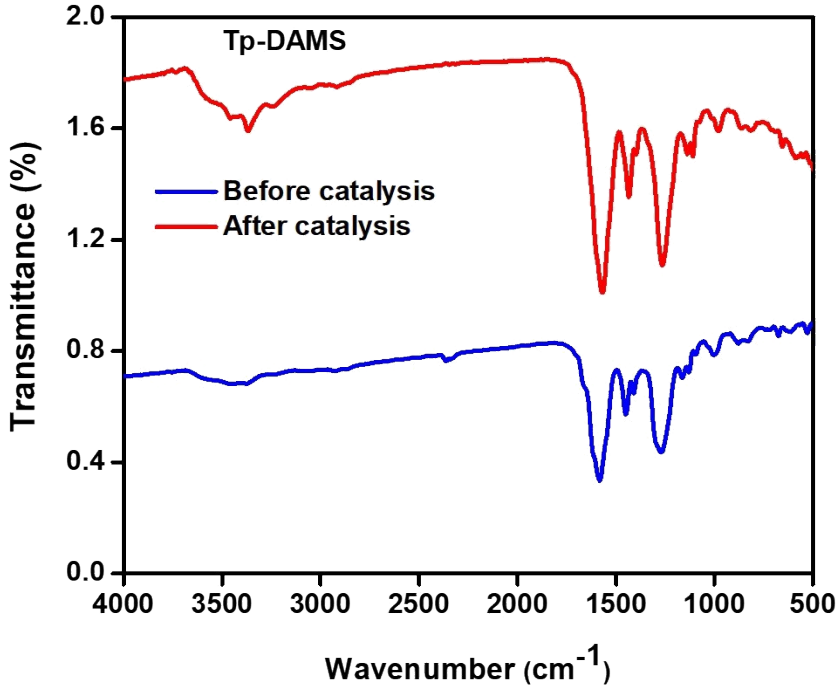

Figure S11. FTIR spectra of Tp-DAMS photocatalyst before and after the catalysis.

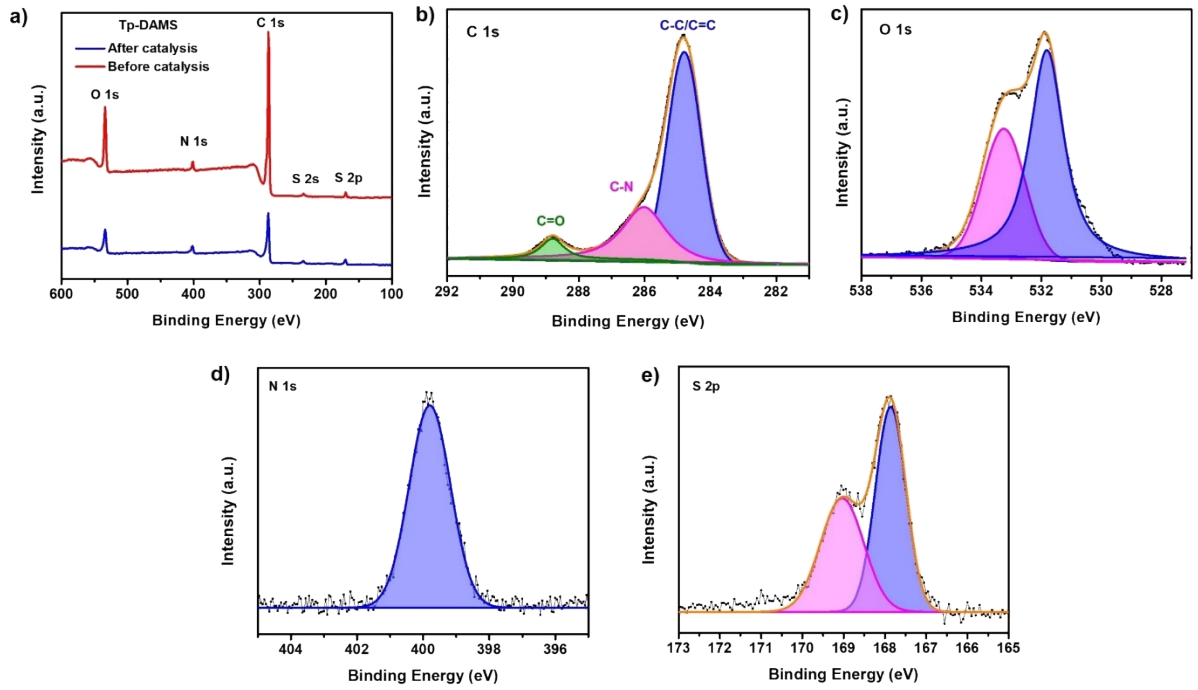

Figure S12. XPS data of (a) Tp-DAMS photocatalyst after and before the catalysis, (b-e) Tp-DAMS COF after the catalysis.

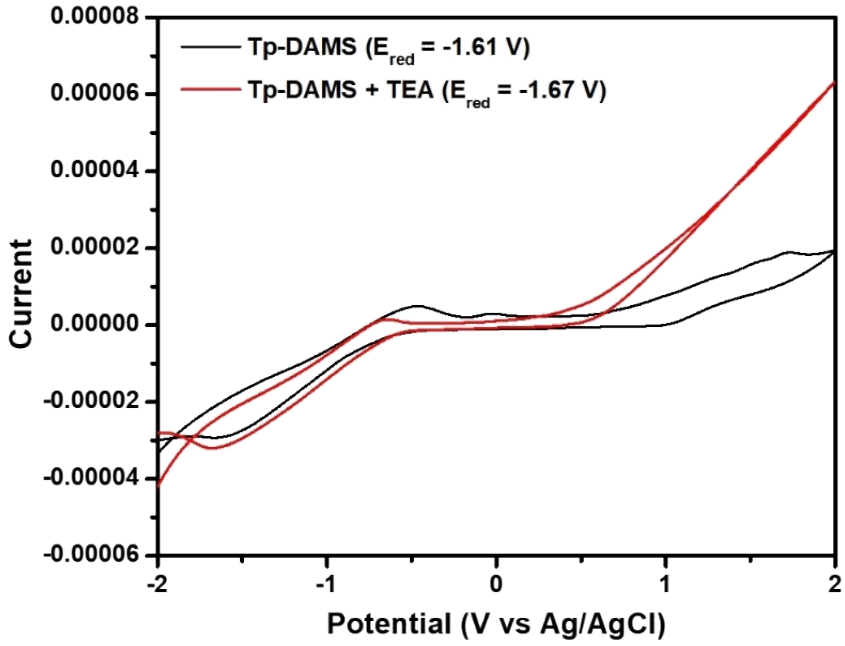

Figure S13. Cyclic voltammetry (CV) of Tp-DAMS photocatalyst with and without TEA in anhydrous DMF containing recrystallized tetrabutylammonium hexafluorophosphate.

^{1}H NMR spectra of synthesized monomer and carboxylic acids

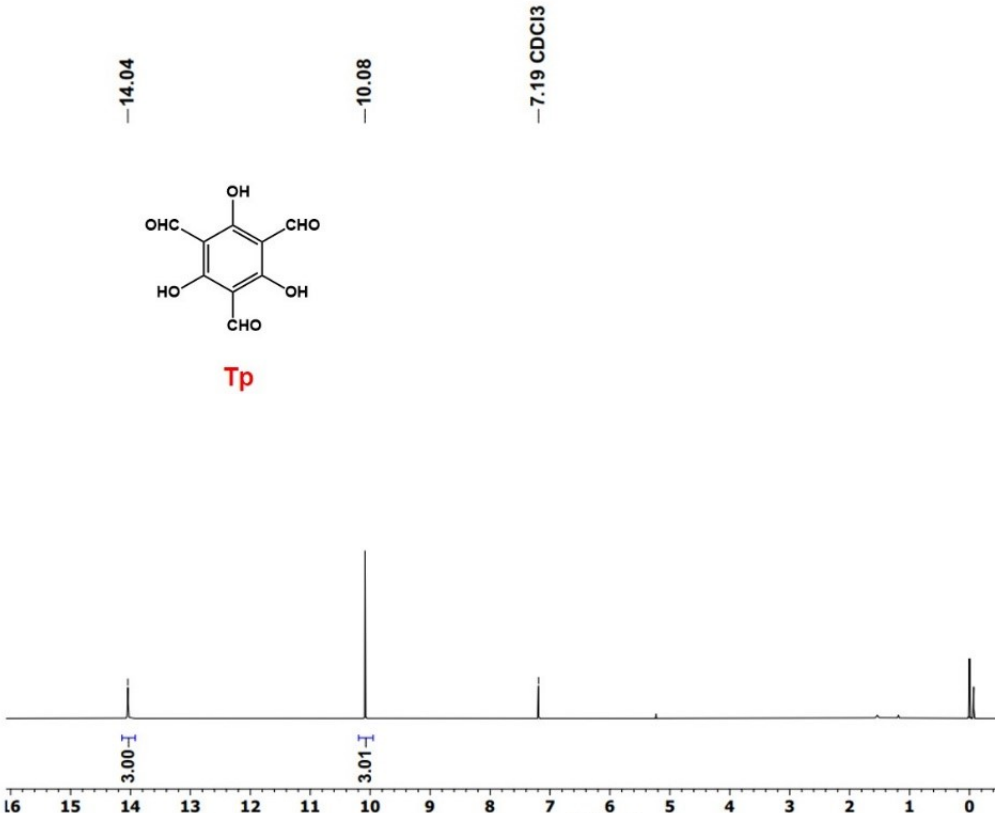

Figure S14. [1]H NMR spectrum of 2, 4, 6-triformylphloroglucinol (Tp). [1]H NMR (500 MHz, CDCl3) δ 14.04 (s, 3H, OH), 10.08 (s, 3H, CHO).

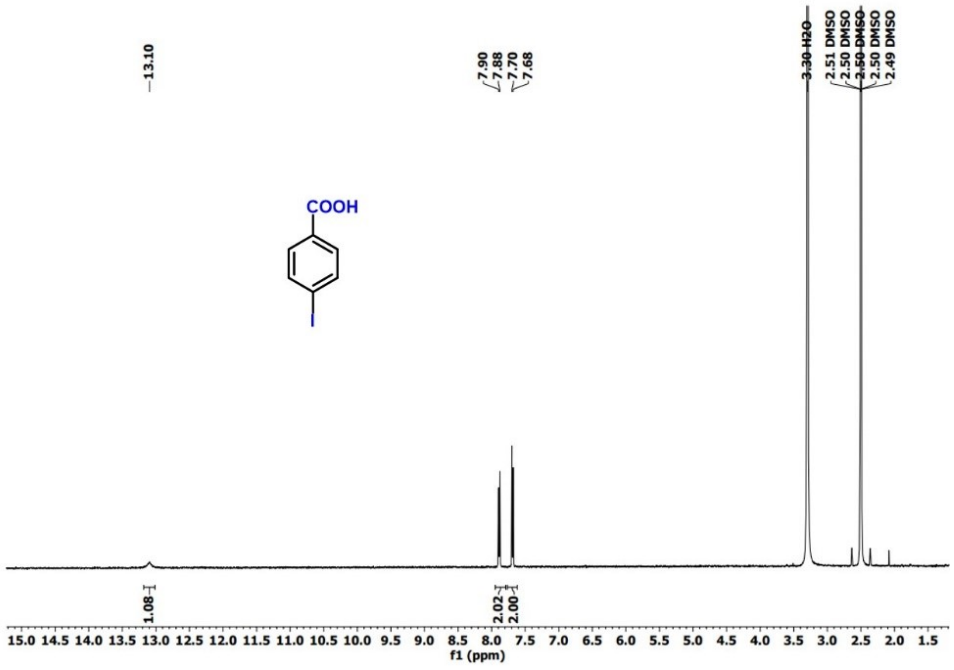

Figure S15. [1]H NMR spectra of 4-iodo benzoic acid. [1]H NMR (DMSO-d6, 500 MHz): δ =

13.10 (s, 1H), 7.90 (d, J = 10.0 Hz, 2H), 7.70 (d, J = 10.0 Hz, 2H).

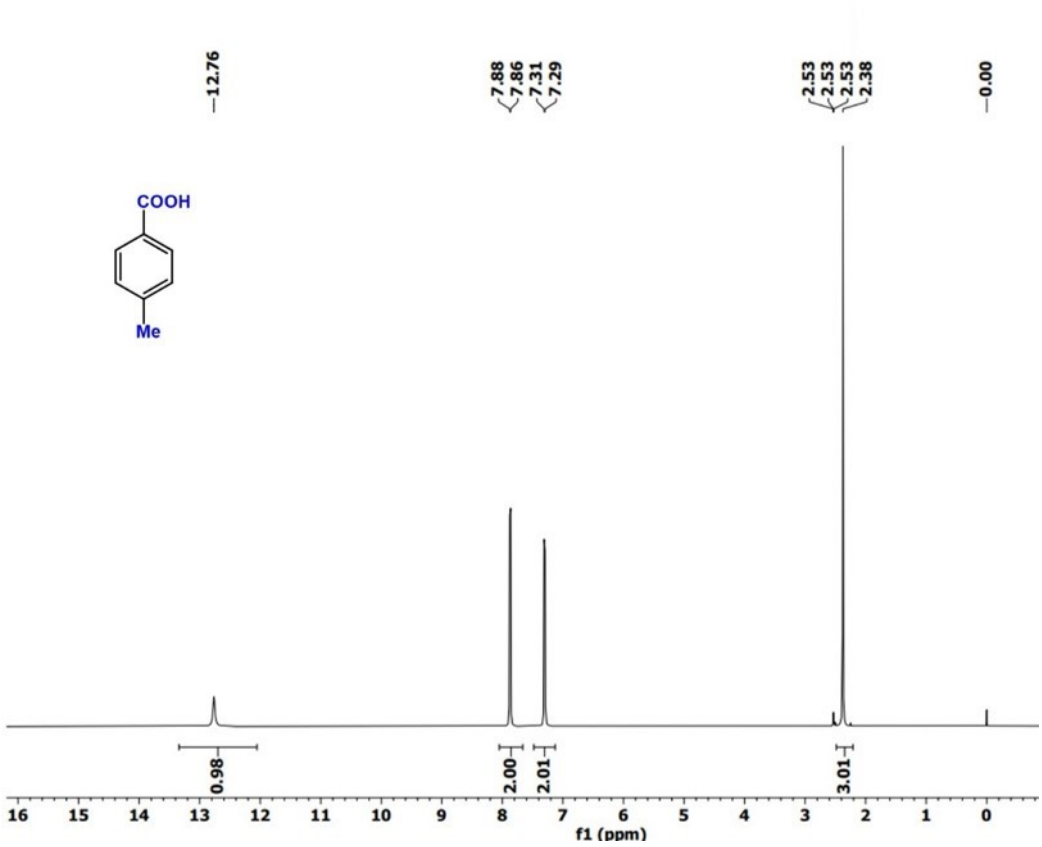

Figure S16. ^{1}H NMR spectra of 4-methyl benzoic acid. ^{1}H NMR (DMSO-d6, 500 MHz): δ = 12.76 (s, 1H), 7.88 (d, J = 10.0 Hz, 2H), 7.31 (d, J = 10.0 Hz, 2H), 2.38 (s, 3H).

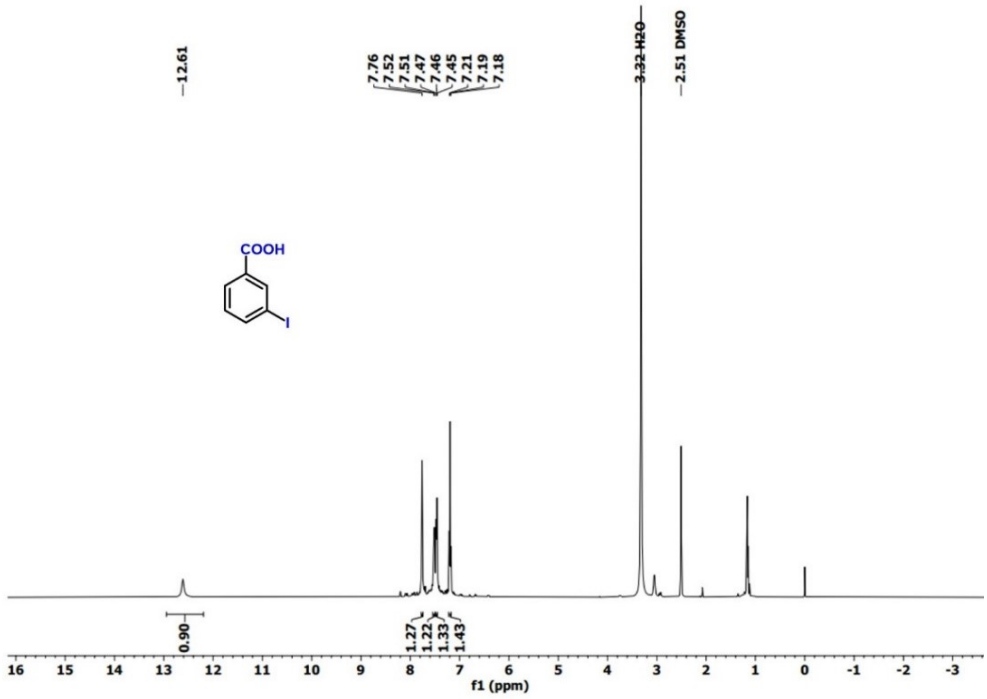

Figure S17. ^{1}H NMR spectra of 3-iodo benzoic acid. ^{1}H NMR (DMSO-d6, 500 MHz): δ = 12.61 (s, 1H), 7.76 (s, 1H), 7.52 (d, J = 5.0 Hz, 1H), 7.47 (d, J = 5.0 Hz, 1H), 7.21 (t, J = 5.0 Hz, 1H).

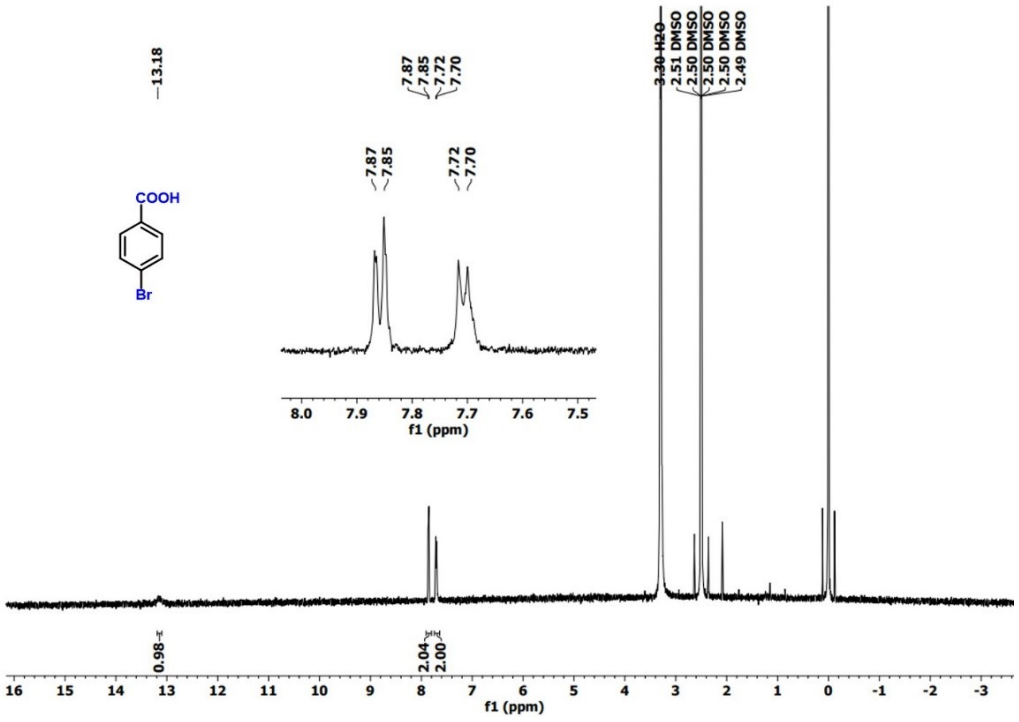

Figure S18. ^{1}H NMR spectra of 4-bromo benzoic acid. ^{1}H NMR (DMSO-d6, 500 MHz): δ =

13.18 (s, 1H), 7.87 (d, J = 10.0 Hz, 2H), 7.72 (d, J = 10.0 Hz, 2H).

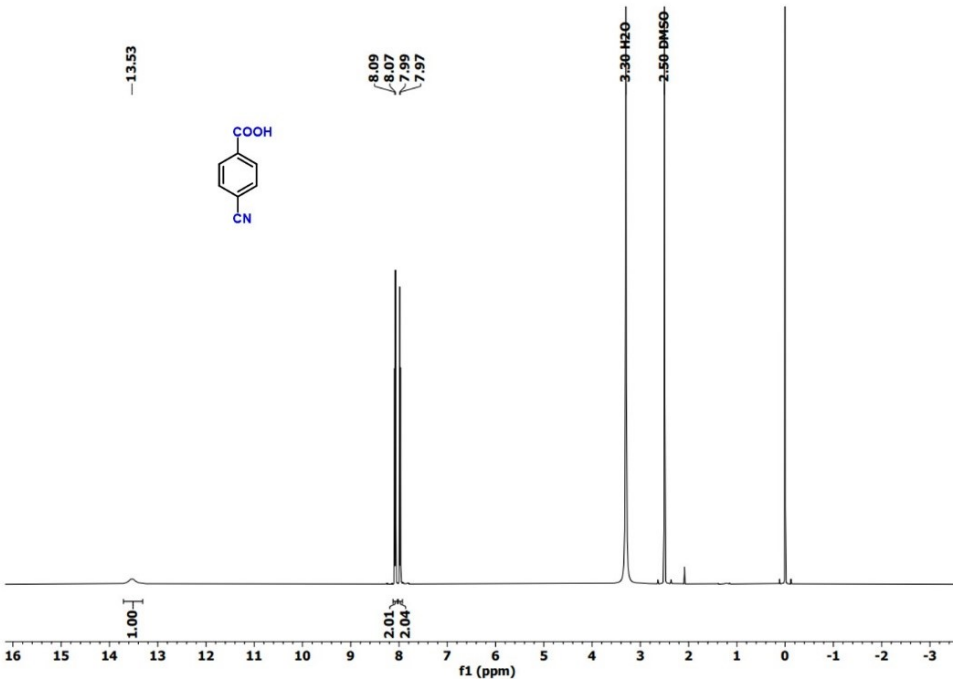

Figure S19. ^{1}H NMR spectra of 4-cyano benzoic acid. ^{1}H NMR (DMSO-d6, 500 MHz): δ 13.53 (s, 1H), 8.09 (d, J = 10.0 Hz, 2H), 7.99 (d, J = 10.0 Hz, 2H).

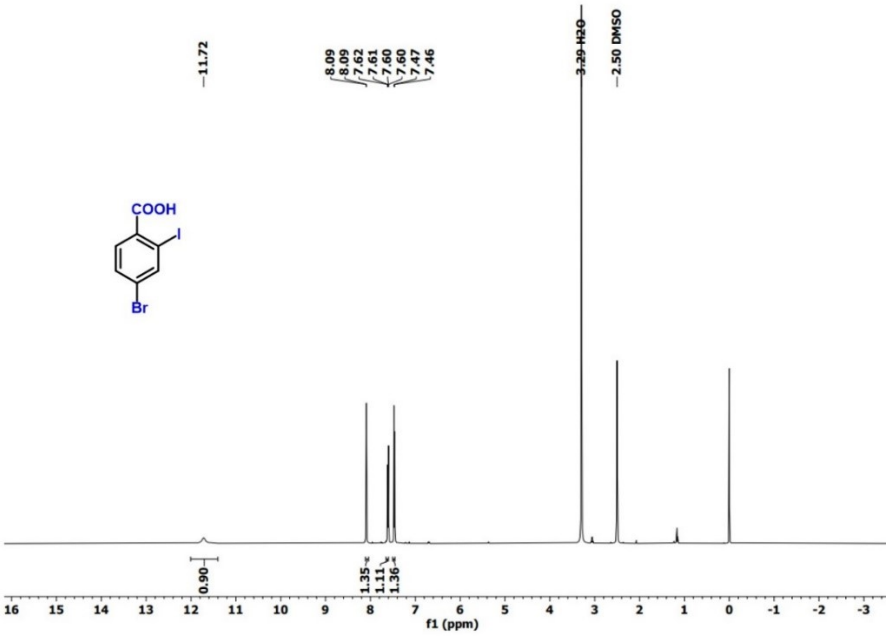

Figure S20. ^{1}H NMR spectra of 4-bromo-2-iodo benzoic acid. ^{1}H NMR (DMSO-d6, 500 MHz): δ 11.72 (s, 1H), 8.09 (s, 1H), 7.62 (d, J = 10.0 Hz, 1H), 7.47 (d, J = 5.0 Hz, 1H).

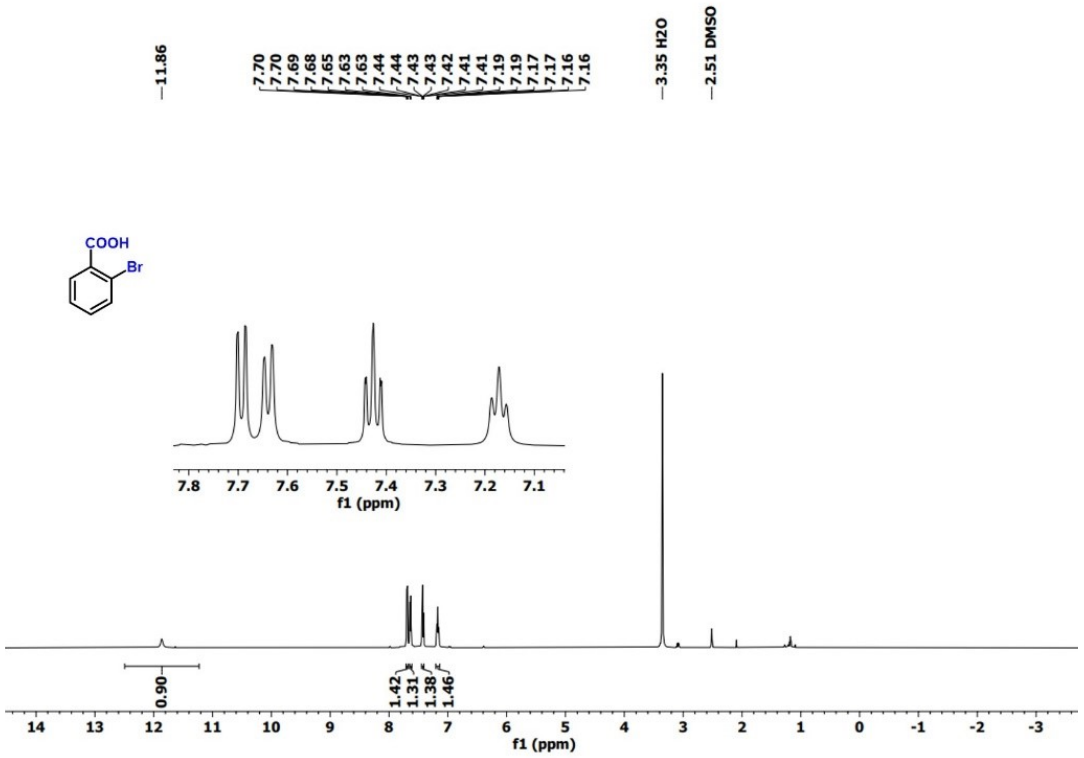

Figure S21. ^{1}H NMR spectra of 2-bromo benzoic acid. ^{1}H NMR (DMSO-d6, 500 MHz): δ 11.86 (s, 1H), 7.70 (d, J = 10.0 Hz, 1H), 7.65 (d, J = 10.0 Hz, 1H), 7.44 (t, J = 20.0 Hz, 1H), 7.19 (t, J = 20.0 Hz, 1H).

Reference

1 A. Jati, K. Dey, M. Nurhuda, M. A. Addicoat, R. Banerjee, B. Maji, *J. Am. Chem. Soc.* 2022, **144**, 7822–7833.

2 Y. A. Stetsiv, M. M. Yatsyshyn, D. Nykypanchuk, S. A. Korniy, I. Saldan, O. V. Reshetnyak, T. J. Bednarchuk, *Polym. Bull.* 2021, **78**, 6251–6265.

3 S. G. Prasad, A. De, U. De, *Int. J. Spectrosc*. 2011, **2011**, 1–7

4 M. G. Faraj, K. Ibrahim, M. H. Eisa, *Roman J. Phys.* 2011, **56**, 730–741